ISSN 0280-5316
ISRN LUTFD2/TFRT--5716--SE

Improving wheel Speed Sensing and Estimation

Christian Trobro
Mathias Magnusson

Department of Automatic Control
Lund Institute of Technology
December 2003

Department of Automatic Control
Lund Institute of Technology
Box 118
SE-221 00 Lund Sweden

Document name
MASTER THESIS

Date of issue
December 2003

Document Number
ISRN LUTFD2/TFRT--5716--SE

Author(s)
Christian Trobro and Mathias Magnusson

Supervisor
Ola Nockhammar, Haldex.
Anders Rantzer, LTH

Sponsoring organization

Title and subtitle
Improving wheel Speed Sensing and Estimation. (Förbättring av hjulhastighetsmätning och estimering).

Abstract
This master thesis project commissioned by Haldex Brake Products AB (in Landskrona, Sweden), and in association with the Department of Automatic Control, Lund Institute of Technology, deals with the problem of correct wheel speed measurements. Investigation into different types of sensors, Inductive-, Hall Effect- and Magneto-Resistive sensors have been carried out, which are sensors that may be used, when measuring the velocity of a wheel. It also looks into different types of methods that can be used to estimate a velocity; zero detection, estimation with few measurements, and tracking demodulation. Problems, such as noise, time demanding calculations and adapting the sensor signal so it may be used in a microcontroller, which could arise when implementing these methods into a microcontroller, are also investigated.
The conclusions are that to obtain wheel speed estimates at low speed sufficiently fast, the information in the sinusoidal signal from the sensors has to be used, and therefore, if one sensor is used, the Few Measurements method is the most appropriate, and if two sensors are used the Tracking Demodulation method. Finally scheduling is suggested, which means that the normal zero detection is used at high speed and the tracking demodulation method is used at low speed.

Keywords

Classification system and/or index terms (if any)

Supplementary bibliographical information

ISSN and key title
0280-5316

ISBN

Language
English

Number of pages
58

Recipient's notes

Security classification

Improving wheel speed sensing and estimation

Master Thesis Students:
Mathias Magnusson, E98
Christian Trobro, E01

Supervisor Haldex Brake Products AB:
Ola Nockhammar
Supervisor Lund University (LTH):
Anders Rantzer
Department of Automatic Control

Table of Content

1. Introduction

In today's automotive systems (such as ABS, ESP etc.), it is of great importance to have well defined and reliable wheel speed signals. Therefore it is very convenient that the sensors, which measure these signals, are robust. This has resulted in sensors with a rather rough resolution, which has been enough in traditional "Bang-Bang" ABS-systems. To make improvements in these systems, much better wheel speed signals are needed. In future systems the intelligence will be moved closer to the wheels, which makes better use of the sensor signals.

This master thesis project commissioned by Haldex Brake Products AB (in Landskrona, Sweden), deals with an investigation whether it is possible to make the present signals from the sensors better? E.g. at low vehicle speed, the today's sensor signal is too weak, and therefore no reliable velocity estimation can be performed. Is it possible to use other wheel speed estimation methods? Is it achievable to make improvements with more advanced signal processing? Is another sensor needed to achieve improvements? Could two sensors be used to obtain better results?

In chapter two the wheel speed sensor in an Anti-Lock Braking System is presented, or more exactly; how this sensor signal is used in an ABS. In the third chapter the general function of wheel speed sensing with a sensor is introduced, and also different kinds of sensors are discussed, and their advantages and disadvantages are shown. The characteristic of the waveform in the sensor signal is brought up in chapter four. In the following chapter, i.e. chapter five, different wheel speed estimation methods, i.e. common zero detection, few measurements method and tracking demodulation method, are introduced. The working principle of these methods, and their advantages and disadvantages are discussed and analyzed. In chapter six disturbances on the attained signals and estimations are lightened, and suggested filtering of these disturbances are introduced. The test rig, on which the estimation methods have been tested, is presented in chapter

seven. In chapter eight, the general implementation ideas of the different estimation methods are discussed and shown. Finally, in chapter nine, the conclusions of this project are presented and summarized.

2. The use of wheel speed measurement in an ABS

The following chapter will investigate how the wheel speed measurement is used in an ABS (Anti-Lock Braking System)[1], and the importance of this speed measurement to be reliable.

2.1. ABS system

A main function of the ABS is to keep the brakes from being jammed. A main idea is to release pressure from the brakes when they are locked up. To control this, a measurement called slip is made. The slip is defined as the relative difference of the circumferential velocity of the driven wheel, $\omega_w r_w$ and its absolute velocity v_w. This gives following statement for the slip[2]:

$$s = \frac{\omega_w r_w - v_w}{v_w} \tag{2.1}$$

The wheel speed v_w may be calculated from the velocity from the two non-driven wheels, assuming that the vehicle has two front wheel drive. This means when the friction slip is -1, the front brakes are locked and the front wheels skid on the surface, a situation that an ABS system will prevent from happening.

A modern antilock brake system is an electronic feedback controller system, which uses the information about the slip to control the brake pressure applied to the brakes. These systems often consist of a sensor that measures the circumferential speed of the wheels. It also consists of an electronic control unit and a pressure modulator to control the brakes. See figure 2.1 for a principle sketch.

[1] For further information see reference [12] and [14].
[2] For further information see reference [14].

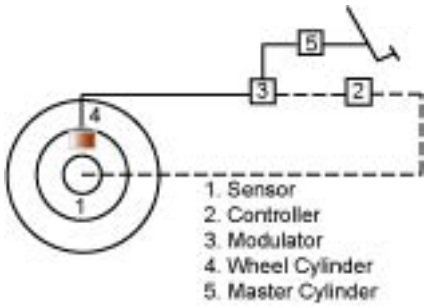

Figure 2.1. Principle sketch for an antilock brake system

The rotation of the tires is normally measured with an electromagnetic pulse pickup that is mounted in the centre of the wheel hub. Depending on the construction of the gear-tooth wheel[3] placed in the wheel hub, it generates 90-100 pulses per wheel revolution (depending on how many teeth the gear-tooth wheel has), and this gives a good base to derive the angular speed and deceleration of the wheel. With this information the control unit then calculates the slip and will then be able to decide if the wheel is about to lock, and if so, it takes proper action and sends a control signal to the modulator, that corrects the pressure to the brakes to avoid locking.

[3] See chapter 3.1.

3. Sensors

This chapter brings up the principle for common velocity measurements with a sensor and a gear-tooth wheel, and also discuss how the signals are obtained in different types of sensors.

3.1. Velocity measurement

The idea when measuring the velocity of a vehicle is that a gear-tooth wheel (also called target wheel) and a sensor are applied on each of the vehicle wheels. The gear-tooth wheel is of ferromagnetic material. When the wheel is moving, the sensor is able to “feel” the changes of the magnetic field between the target wheel and a permanent magnet in the sensor. The sensor is detecting and transforming the variation in flux level to an output voltage. The frequency of this output voltage is proportional to the wheel frequency.

How this signal is obtained differs between different types of sensors. In this and the following chapter the main idea for Inductive-, Hall-Effect- and Magneto-Resistive sensors are discussed.

3.2. Working principles of Inductive sensors

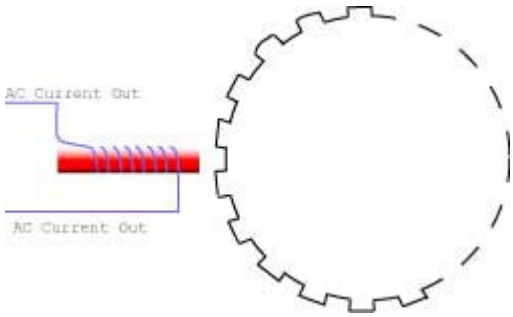

Figure 3.1. Principle sketch for inductive sensor with target wheel.

In figure 3.1 the principle appearance for an inductive sensor with a gear-tooth wheel is shown. The sensor set up is shown in figure 3.2. The magnetic field ($\overline{B}$) acting on the coil in the sensor is shown in figure 3.3.

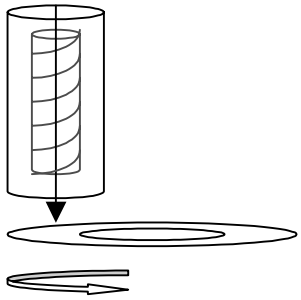

Figure 3.2. Sensor setup in proportion to the target wheel

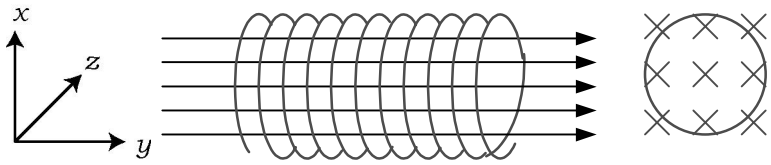

Figure 3.3. Magnetic field acting on the coil

The output voltage from the sensor is given by

$$e(t) = \frac{d\Psi}{dt} = -\frac{d}{dt}\left[\sum_{i=1}^{N}\varphi_i\right] \tag{3.1}$$

where Ψ is the total flux linkage and φ_i is the flux linkage in one of the N windings of the coil. Neglecting the flux leakage, the uniform flux linkage Φ in the magnetic core is

$$\Phi = \varphi_i = \int_A B(\sigma)d\sigma \tag{3.2}$$

where A is the cross section of the core. If the core is rectangular with length L in the y-direction, then

$$\Phi = L\int_{\theta(t)}^{\theta(t)+\delta} B(\alpha)R\cdot d\alpha \tag{3.3}$$

where $\theta(t)$ is the location of the target wheel at time t when it is above the

core, δ is the width of the core in the θ-direction and R is the radius of the target wheel. Eq. (3.1) – (3.3) give

$$e(t) = -NLR\frac{d}{dt}\int_{\theta(t)}^{\theta(t)+\delta} B(\alpha)\cdot d\alpha = -NLR\frac{d\theta}{dt}\frac{d}{d\theta}\int_{\theta(t)}^{\theta(t)+\delta} B(\alpha)\cdot d\alpha \qquad (3.4)$$

If the wheel has constant velocity, i.e. $\frac{d\theta}{dt} = \omega$ then

$$e(t) = -NLR\omega\frac{d}{d\theta}\int_{\theta(t)}^{\theta(t)+\delta} B(\alpha)\cdot d\alpha = -NLR\omega[B(\theta+\delta) - B(\theta)] \qquad (3.5)$$

From this equation it is seen that the amplitude of the voltage is proportional to the velocity of the wheel[4]. Therefore a weaker signal (lower SNR[5]) for small velocities for the Inductive sensor is given. This results in the need of some sort of filtering and amplification of the signal, before velocity estimation can be performed. Also it says from eq. (3.5) that the amplitude becomes large for high velocities. To show that eq. (3.5) is valid the test rig[6] has been run with an inductive sensor at different velocities. See figures 3.4.

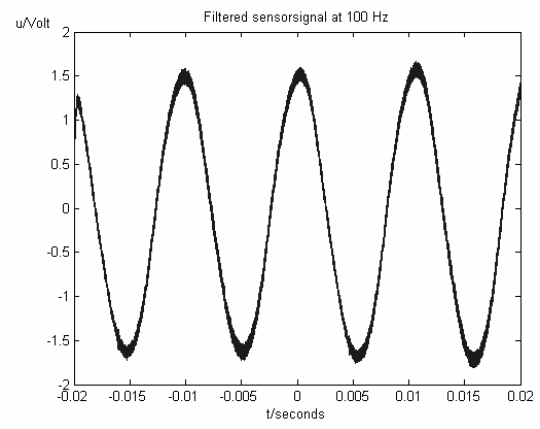

Figure 3.4a. Sensor frequency at 100Hz.

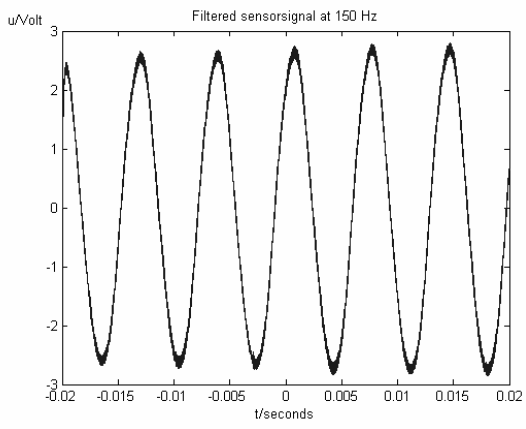

Figure 3.4b. Sensor frequency at 150Hz.

[4] See reference [6].
[5] SNR=Signal to noise ratio
[6] Information about the test rig is presented in chapter 7.

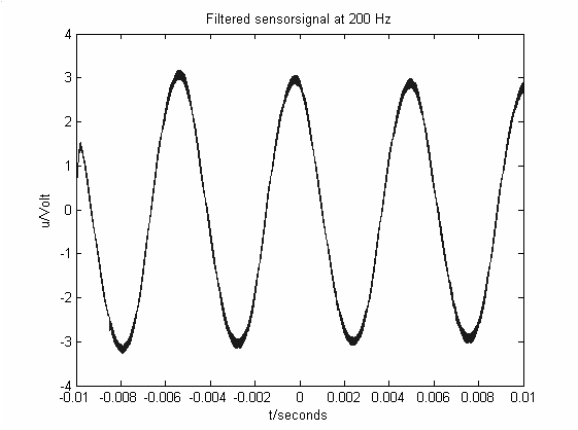

Figure 3.4c. Sensor frequency at 200Hz.

In figure 3.4 it is shown that for different sensor frequency, different amplitude of the signal is given, and therefore eq (3.5) is valid.

3.3. Working principles of Solid-state sensors (Hall-Effect- and Magneto-Resistive sensors)

3.3.1. Main idea

When applying a semiconductor (Hall- or Magneto-Resistive element) to a stationary magnet, an electrical signal $v(t)$ is obtained, which varies in time according to the wheel speed. This signal $v(t)$ is

$$v(t) = f[B(\theta)] \tag{3.6}$$

where $\theta(t)$ is the position of the semiconductor at a certain time t and $f(B)$ is the characteristic of the semiconductor. The semiconductor and the magnet together form a Solid-state sensor.

In chapter 3.3.2 it is shown that for a Hall-effect sensor, the output signal is dependent on the size of the semiconductor but independent of the velocity of the wheel. This conclusion is also valid for Magneto-Resistive sensors[7]. Depending on the rotation speed of the wheel, the flux will vary because the

[7] For further information see reference [4].

magnetic field will bend different ways, due to the position on the target wheel. Bending characteristics of the magnetic field also occurs when the wheel is stationary. The magnet generates a stationary flux, which provides an output signal on the sensors; due to the fact that the sensor needs a supply voltage to be able perform a signal. Therefore it is possible to measure very slow velocities. (Inductive sensors can only measure the variations in the flux and are therefore unable to perform reliable output signals for low velocities).

3.3.2. Hall-effect sensor

The output signal from a Hall-effect sensor is a voltage signal. Consider figure 3.5.

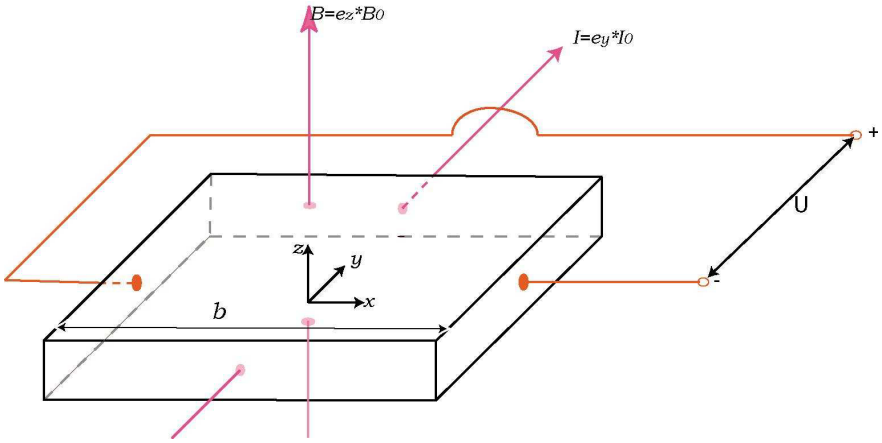

Figure 3.5. Principle of the Hall-Effect.

What is seen in figure 3.5 is a thin plate of a semiconductor material. Through the plate a current is sent in the y-direction. Due to the magnetic field of the permanent magnet in the z-direction, the charge carriers (suppose they are electrons) will move in the x-direction of the plate. According to Lenz's law[8], further movements are counteracted by the electric field, which the movements resulted in. The arising state of equilibrium is,

$$\overline{E}_h = -\overline{v} \times \overline{B} \qquad (3.7)$$

[8] Lens' law states that whenever there is an induced electromotive force (emf) in a conductor, it is always in such a direction that the current it would induce would act in opposition to the change, which caused the induced emf.

where $\bar{E}_h$ is the electrical field, $\bar{v}$ is the velocity of the charge carriers and $\bar{B}$ is the magnetic field. From figure 3.4 it is seen that the velocity of the electrons is

$$\bar{v} = -\bar{e}_y \cdot v_0 \tag{3.8}$$

and the electrical field is then

$$\bar{E}_h = -(-\bar{e}_y v_0) \times \bar{e}_z B_0 = \bar{e}_x v_0 B_0 \tag{3.9}$$

The Hall voltage over the plate is given by[9]

$$V_h = -\int_0^b E_h dx = v_0 B_0 b \tag{3.10}$$

where b is the width of the plate. In eq. (3.10) it is shown that the output voltage is dependent on the size of the semi-conductor, and the amplitude of the output signal is independent of the wheel speed[10], as stated before.

The current I through the plate can be written as

$$\bar{I} = n \cdot q \cdot \bar{v} \tag{3.11}$$

where n is the number of free charge carriers q per volume unit, which move through the plate. The ratio

$$\frac{E_x}{I_y \cdot B_z} = \frac{1}{n \cdot q} \tag{3.12}$$

is called the Hall coefficient[11] and is different for different materials, i.e. different sensors. This means that the output is different for different types

[9] See reference [3].
[10] See reference [6].
[11] See reference [3].

of sensors (and slightly differ from sensor to sensor). Therefore when, for instance two Hall Effect sensors are used in a wheel speed measurement, the amplitude of the sensor signals could differ, which could cause problems in the wheel speed estimation.

3.3.3. Magneto resistive sensor

Due to the magneto resistive effect[12], resistance variation may be measured in a Magneto resistive sensor. Depending on the rotation speed of the wheel, the resistivity will vary proportional to the wheel speed. Note that the amplitude of the output signal is independent to the wheel speed. With a Magneto-Resistive sensor, larger output signals are achieved (larger SNR) compared to a Hall-Effect- or an Inductive sensor[13]. On the market there are companies which have been doing research on magneto-resistive sensors, but have not come to a final solution. Therefore further investigation on the Magneto-Resistive sensor is not done in this rapport.

3.4 Summary

In this chapter it is shown that the amplitude of the inductive sensor signal is proportional to the wheel speed, which means that the SNR becomes low at slow wheel speed. The signal of the Solid-State sensors is instead independent of the wheel speed, which means more reliable signals are obtained at low velocities.

[12] The property of a current carrying a magnetic material to change its resistivity, in the presence of an external magnetic field.
[13] See reference [4].

4. The Sensor signal

The characteristics of the sensor signal for different appearance of the target wheel, and a discussion of embedded signal processing in common Solid-State sensors, are brought up in this chapter.

4.1. Waveform characteristics

The appearance of the output signal of the different sensors has some factors in common, but also some differences. In this chapter these factors are discussed.

First an approximation of the magnetic field formed between the permanent magnet and the target wheel is made, i.e.

$$\overline{B} = \mu_0 \cdot B_1 \cdot f(t) \cdot \overline{e}_\varphi \quad , \quad B_1 = \left(1 - \frac{a}{a_{max}}\right) \cdot B_0 \tag{4.1}$$

In eq (4.1), $f(t)$ is how the magnetic field varies in time. B_0 and μ_0 are magnetic constants and $\overline{e}_\varphi$ is the direction of the magnetic field. The space between the top of the sensor and the surface of the target wheel is described with *a* and *amax*. The value of *a* is the space currently used and *amax* is the space that could be used and still achieve a signal that could be detected. This ratio is constructed with the knowledge that the strength of the electromagnetic field will decay when the space between sensor and target wheel rises[14].

The output voltage from the sensor becomes

$$u(t) = g(\overline{B}) \tag{4.2}$$

where the function g is different for the different types of sensors.

[14] This conclusion can be drawn from chapter 6.2, about the wobble disturbance, which shows that different spacing between the sensor and target wheel will result in differences in signal amplitude, when running at constant velocity.

Conclusion of the output waveform is made[15], i.e. the function f from eq. (4.1) will be dependent on the angular velocity of the wheel and the geometry of the target wheel, such as space between teeth on the wheel, width and appearance of the teeth. How the output voltage will be affected by different constructing parameters of the target wheel is shown in figure 4.1.

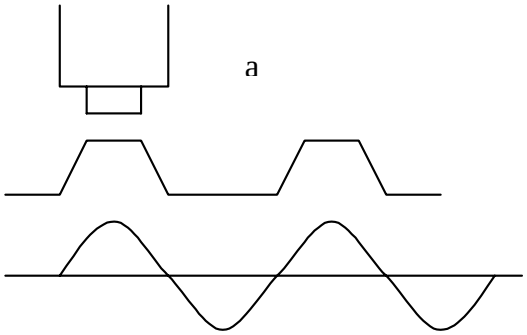

Figure 4.1a. Even spacing and even teeth.

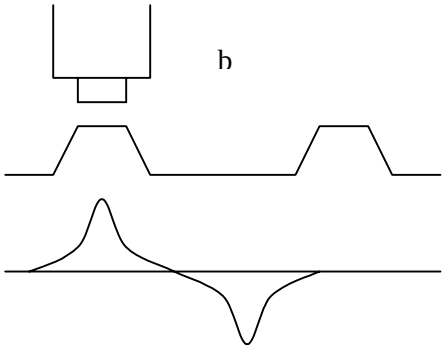

Figure 4.1b. Large spacing, even teeth.

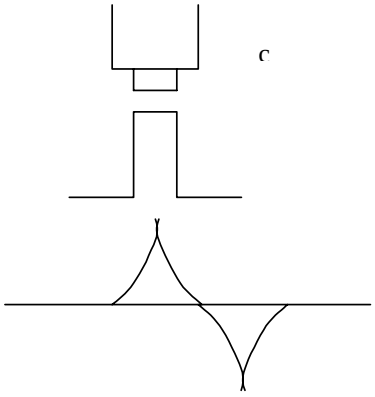

Figure 4.1c. Large spacing, narrow teeth

In figure 4.1a it is shown that with an even width and gap between the teeth, a sinusoidal output waveform is given.

As seen in figure 4.1b an increased gap between the teeth results in an exponential raise and fall of the output waveform. The output waveform has its maximum around the middle of each tooth and its minimum value in the middle between the teeth. For the Inductive sensor the maximum amplitude is still dependent on the angular velocity.

[15] See reference [2]

As seen in figure 4.1c, a narrow tooth with large spacing between each following tooth will decrease the raise/fall time in the waveform, and also shorten the signals negative output value after a tooth has past.

In chapter 5 different estimation methods of the wheel speed are discussed. Some of the methods are based on different waveforms of the sensor signal. Therefore the construction of the target wheel is important.

4.2. Embedded Signal processing

On today's market when a Solid-State sensor together with a Ferro-magnetic target wheel is used as the speed estimator, an embedded electronic circuit is added[16]. This is done because of the need of a supply voltage for the Solid-State sensors. In the electronic circuit a transformation of the sensor signal to a pulse-train signal is made. This pulse-train signal changes between zero and high state when the sensor passes a target wheel tooth. In figure 4.2 an output signal from a Hall-Effect sensor[17] is shown.

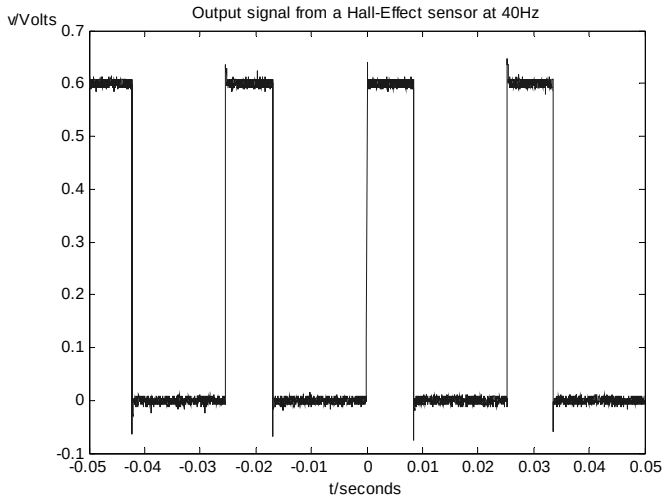

Figure 4.2. Output signal of a Hall-Effect sensor at 40Hz.

In figure 4.2 the test rig[18] has been run so that the sensor frequency is 40Hz[19]. It is also seen that the high-state pulse width is shorter than the

[16] See reference [5].
[17] Honeywell 1GT101DC sensor. See reference [5].
[18] The test rig is presented in chapter 7.
[19] For transformation from sensor frequency to vehicle speed, see chapter 5 and Appendix A.

lower state, because the target wheel on the test rig has got larger space than teeth, see figure 4.1b.

An advantage with the pulse modulator circuit is that more reliable wheel speed estimations can be made. The velocity estimation is made by measuring time in between two rising flanks, i.e. the period time of the sensor signal. A problem occurs when driving at low speed. If there are time demands on the velocity estimator, i.e. a new estimated wheel speed has to be made within a defined time. Then if the period time of the sensor signal is more than the demanded estimation time, this will result in missed deadlines. For instance, the fastest estimation time for the wheel speed in the example in figure 4.2 is around 25ms. That is one of the reasons why another estimation procedure is needed for low speed.

4.3 Summary

Different waveform characteristics are achieved by the sensors for different appearances of the target wheel. To obtain a sinusoidal signal even spacing between teeth and gaps are needed, which is appropriate for the estimation methods described in chapter 5. (See footnote nr. 20.)

Common Solid-State sensors have embedded signal processing, due to their need of a supply voltage. This signal processing transforms the signal to a pulse-train, and therefore a more reliable output signal is achieved. At low velocities a problem occurs, which is that its velocity estimation procedure cannot perform a new estimate if there are time demands on it. Therefore the original sensor (without embedded signal processing) is needed, to estimate wheel speeds at low velocities more often.

[20] More exactly, Few Measurements- and Tracking Demodulation method.

5. Different velocity measurement methods

In this chapter different wheel speed estimation methods are discussed and analyzed. These methods are zero-detection, few measurements method and tracking demodulation method, where the first two methods use one sensor, and the last uses two sensors to estimate the velocity. But first a clarification of how much a sensor frequency is in vehicle speed.

The frequency of the sensor signal is, as mentioned, proportional to the wheel speed. When determining the speed of the vehicle, a transformation from the frequency of the sensor has to be made. Assuming the sensor frequency is f_s, the vehicle speed is v_v, the number of teeth on the target wheel is N, the vehicle wheel radius r_v and the vehicle wheel circumference is o_v. The vehicle speed is then

$$v_v = \frac{o_v}{N} \cdot f_s = \frac{2 \cdot \pi \cdot r_v}{N} \cdot f_s = k \cdot f_s \qquad (5.1)$$

If $r_v = 0.5\text{m}$ and $N = 96$ the transformation factor k equals $3.3 \cdot 10^{-2}\,\text{m}$. (See footnote nr. 21). In this chapter, step responses in sensor frequency are investigated. To understand in which vehicle speed range the step responses take place, see Table A.I in Appendix A.

5.1. Using one sensor

5.1.1. Frequency estimating using zero detection

When simulating with a normal sinusoidal it is easy to calculate the frequency by detecting every zero crossing, and calculating the time in-between zeroes. This is actually how the velocity estimation is done in

[21] An approximation of the radius of a truck wheel is 0.5m, and the number of teeth on the target wheel of Haldex Brake Products is 96.

today's system, both with an Inductive sensor or a Hall Effect sensor. The Simulink simulation is shown in figure 5.1.

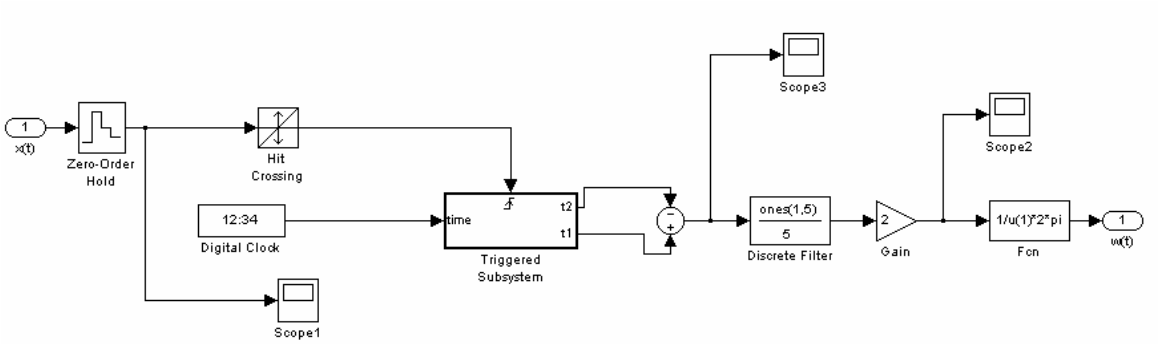

Figure 5.1. Simulink model of zero detection.

A continuous signal is sent into this simulation where it is sampled by the first block. The sample time is put to appropriate levels to avoid aliasing[22]. The next block simply checks if the signal is zero, to broaden this; a small hysterises has been put into this block. This means that the Hit Crossing interprets all signals inside ±a volt as a 0, and then output a Boolean 1. This will give a more stable and easy way to detect zero detection; it will also be less sensitive to noise. Every rising and fall flank is detected and used to trigger the Triggered Subsystem, which calculates the time between two following rising and fall flanks. This is then half of the period time. The triggered subsystem is shown in figure 5.2.

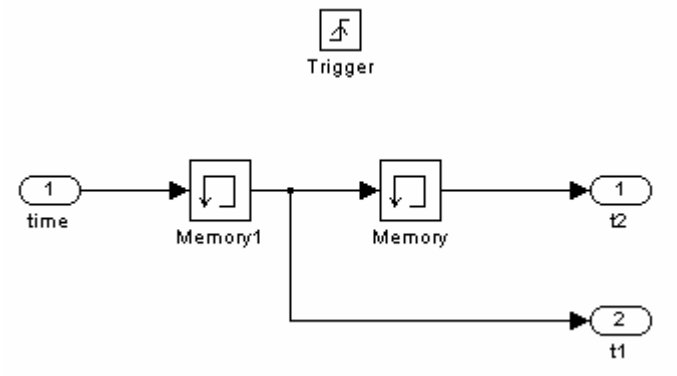

Figure 5.2. Triggered subsystem

[22]The sample frequency has to be at least twice the signal frequency (also called the Nyquist frequency) to avoid aliasing. See reference [15].

To give a more stable value of the frequency, a mean value of measured half period times are read, and then a value of the frequency is calculated.

A simulation with sinusoidal input gives the output shown in figure 5.3. The output signal has been cut before t = 1.5 seconds, because it did not give any correct value. This because the triggered subsystem needs two zero crossings. That means that it will take a period before it may output a correct value. See figure 5.3.

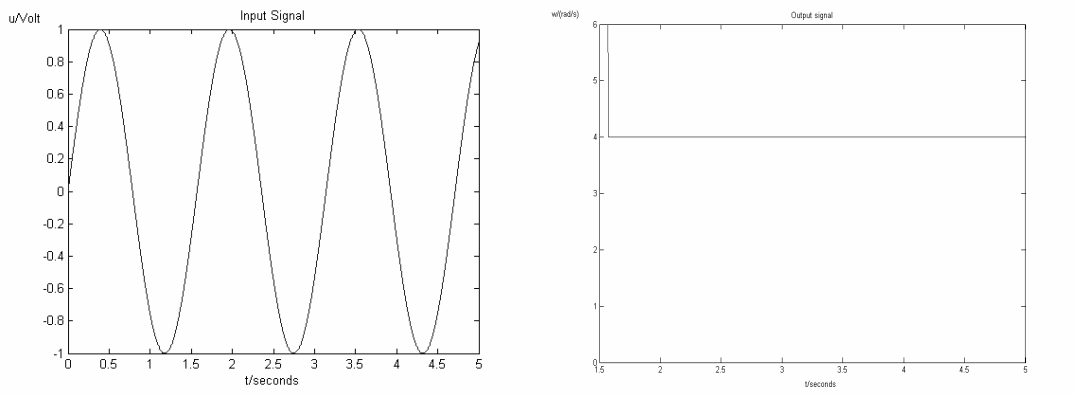

Figure 5.3. Sinusoidal input with corresponding frequency estimation.

The sinusoidal has a frequency of 4 rad/s, and as seen in figure 5.3, the output signal in the zero crossing detection gives this frequency output. A problem that may arise when the frequency rises is that the sample time is too low, and a correct and stable output is not given. By changing to a higher sampling frequency (as stated before it has to be at least twice the frequency of the input signal), this could be solved.

The big advantage of this system is that it will be able to calculate the frequency, even if the input signal undergoes big changes as for example, if narrow target teeth are used with an even spacing between the teeth. The input signals derived in figure 4.1c in chapter 4.1 will give the result shown in figure 5.4 with a sensor frequency of 6 rad/s. This example gives an accurate output signal because it measures the time between each zero crossing.

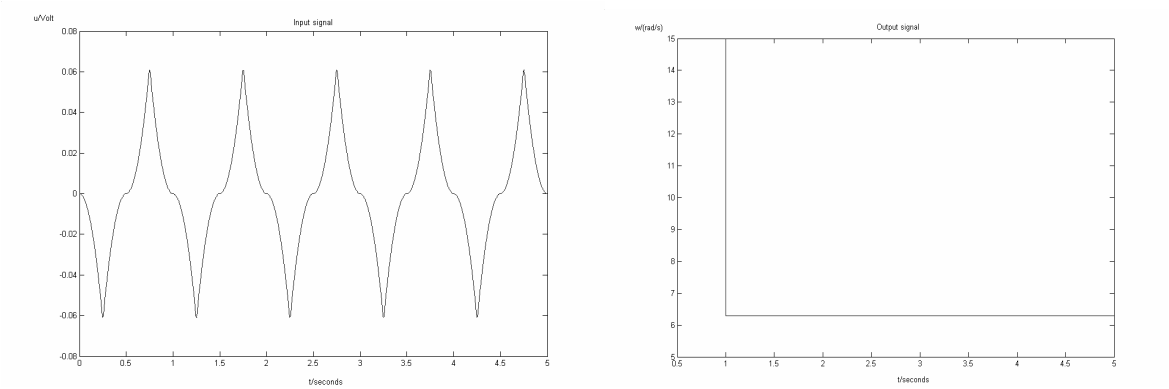

Figure 5.4. Zero detection with no sinusoidal input.

A signal with large spacing between teeth will not give a correct result at once, the model has to be changed a bit to solve this because the zero crossing takes longer time than in the examples shown above, hence a cross level ±a volt has to be used.

All the models in this chapter have been simulated without any noise added to the signal. If noise is introduced into the system, an effective filter, e.g. ARMA-filter or analogue LP-filter[23], has to be used before the signal is put into the zero crossing detection, this to avoid faulty zero detection. It might also be wise to use a larger offset to detect zero because the signal is very noise sensitive around 0 volts and by changing the offset voltage the sensitivity is reduced.

5.1.2. Few Measurements method

This method[24] is a fast method for determining the frequency for a single sinusoid, i.e.

$$x(t) = A \cdot \cos(\omega \cdot t + \theta) \qquad (5.2)$$

If this signal is sampled with the sample time h (h is chosen to avoid aliasing), at time t = [0, h, 2h] will result in following samples:

[23] See chapter 6 for these filter descriptions.
[24] See reference [1]

$$\begin{aligned} x[0] &= A \cdot \cos(\theta) \\ x[1] &= A \cdot \cos(\omega \cdot h + \theta) \\ x[2] &= A \cdot \cos(2 \cdot \omega \cdot h + \theta) \end{aligned} \tag{5.3}$$

If

$$r = \frac{x[0] + x[2]}{2 \cdot x[1]} \tag{5.4}$$

and using the trigonometrically equations

$$\begin{bmatrix} \cos(a + b) = \cos(a) \cdot \cos(b) - \sin(a) \cdot \sin(b) \\ \sin(2 \cdot a) = 2 \cdot \sin(a) \cdot \cos(a) \\ \cos(a) = 2 \cdot \cos^2(a) - 1 \end{bmatrix} \tag{5.5}$$

it can be shown that[25]

$$r = \cos(\omega \cdot h) \tag{5.6}$$

It can be seen when eq. (5.4) is analyzed small values of x[1], i.e. close to zero, small disturbances have large effect and the estimate of r becomes too high. Compensation can be made for this problem by adding zero-crossing detection, which means no sampling takes place close to zero. Another problem is if ω is small, which can give an over-sampled signal if h has such a value that it takes more than 12 samples per period. This will result in that r is close to the absolute value 1, and this error could give values outside the range of cosine $[-1, +1]$. A problem like this can be solved by changing the sample rate for different ω, so the three samples are taken during a quarter of the period of the signal.

[25] For proof, see appendix B.1.

An alternative with Few Measurement is to use one more sample x[3] and compute two cosine estimates[26], i.e.

$$r_1 = \frac{x[0]+x[2]}{2 \cdot x[1]}; r_2 = \frac{x[1]+x[3]}{2 \cdot x[2]} \qquad (5.7)$$

which are not statistically independent and their variances and covariance are

$$\sigma_1^{\,2} = \frac{(0{,}5+r^2)\cdot\sigma^2}{(x[1])^2}; \quad \sigma_2^{\,2} = \frac{(0{,}5+r^2)\cdot\sigma^2}{(x[2])^2}; \quad \sigma_{12} = -\frac{r\cdot\sigma^2}{x[1]\cdot x[2]} \qquad (5.8)^{27}$$

To estimate r, a weighted average is made, i.e.

$$r = \frac{a\cdot r_1 + b\cdot r_2}{a+b}, \text{ where } a = \sigma_2^{\,2} - \sigma_{12} \text{ and } b = \sigma_1^{\,2} - \sigma_{12}. \qquad (5.9)$$

A comparison of these two methods has been run in Simulink and the result is shown in figure 5.4. Real sensor data from an inductive sensor has been used as input data. The frequency on the test rig[28] is 300Hz and a frequency estimate is produced every fifth millisecond. This estimate is an average of all the moment values calculated during the last five milliseconds.

[26] See reference [1].
[27] For variances and covariance estimations see reference [1].
[28] Further about the test rig in chapter 7.

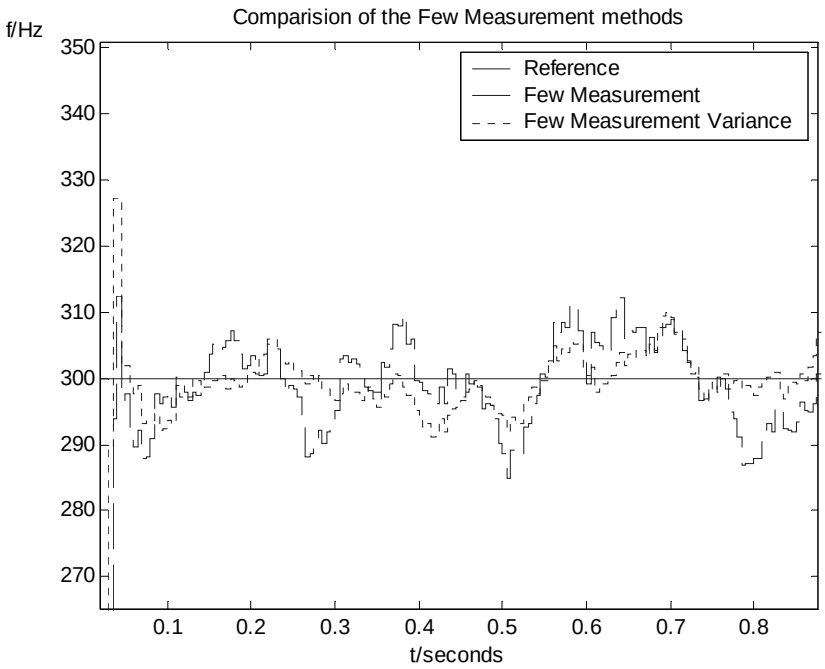

Figure 5.4. Comparison of the two Few Measurement methods.

As seen in the figure, the variance method (after it has been stabilized) is a bit better reducing the wobble[29], which is the main reason why the estimates fluctuate around the correct value. A disadvantage is that it is more complex and therefore takes more time to calculate when implemented.

To summarize, the sample time h has to be faster than the Nyquist Frequency and not make more than 12 samples per period. An optimum is around three samples over a quarter of the period. The advantage with Few Measurement is that it is possible to get velocity measurements more often than zero detection, due to the fact that it calculates a velocity after ¼ of a period, and then a new one every $\frac{1}{12}$ period (compared to the zero detection methods which needs at least ½ a period[30]). One improvement is to add a fourth sample and compute two estimates, calculate their statistics and then estimate a cosine value. This will give a better average value.

[29] The term wobble is explained in Chapter 6.2.
[30] Half a period is enough, if even spacing between gaps and teeth are used. See figure 4.1.

5.2. Using two sensors

It could be of great interest to investigate whether a good estimate of the wheel speed can be obtained using two sensors. One way is a method called "Tracking Demodulation" method[31].

5.2.1. Tracking Demodulation method

It should be possible by using trigonometrically relations to track the signal and therefore estimate the wheel speed when using two sensors. If one of the signals has a phase lag of 90 degrees, one sinusoid and one cosine signal is obtained. See figure 5.5.

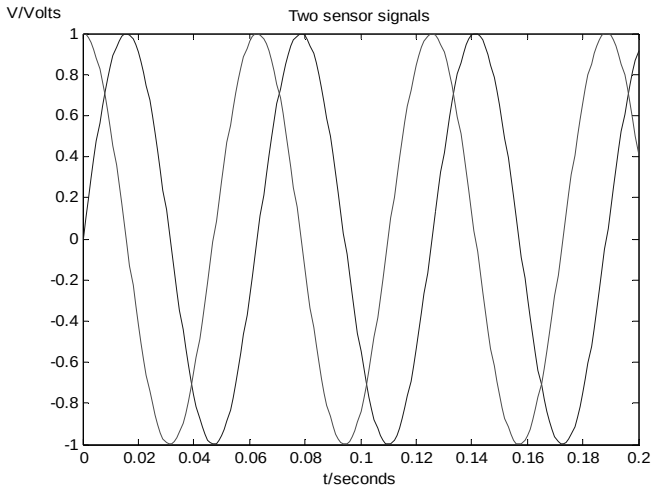

Figure 5.5. Output signal using two sensors.

Using the trigonometrically relation

$$\sin\left(\theta - \hat{\theta}\right) = \sin\theta \cdot \cos\hat{\theta} - \cos\theta \cdot \sin\hat{\theta} \qquad (5.10)$$

where θ and $\hat{\theta}$ are the correct- and the estimated position respectively, an estimation error can be obtained.

[31] See reference [10].

In figure 5.6 a model is shown consisting of a PI-controller followed by an integrator and closed by a feedback loop, which tracks the speed and position.

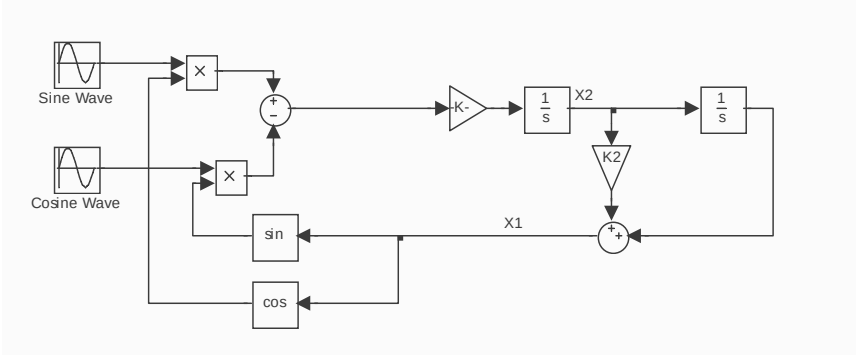

Figure 5.6. Block model for the Tracking Demodulation.

From figure 5.6 it is seen that state X1 is the estimated position of the wheel, and state X2 is the estimated wheel speed. By studying the model in this figure, following steps could be taken to set up a state space model of the Tracking Demodulation.

$$\begin{cases} x_1 = K_2 \cdot x_2 + \dfrac{1}{s} \cdot x_2 \\ x_2 = \dfrac{1}{s} \cdot K_1 \cdot \sin(\theta - \hat{\theta}) \Rightarrow \begin{bmatrix} x_1 = \hat{\theta} \\ x_2 = \dot{\hat{\theta}} \end{bmatrix} \Rightarrow \begin{cases} \dot{x}_1 = K_2 \cdot \dot{x}_2 + x_2 \\ \dot{x}_2 = K_1 \cdot \sin(\theta - x_1) \Rightarrow \\ y = x_1 \end{cases} \\ y = x_1 \end{cases} \tag{5.11}$$

$$\Rightarrow \begin{cases} \dot{x}_1 = K_1 \cdot K_2 \cdot \sin(\theta - x_1) + x_2 \\ \dot{x}_2 = K_1 \cdot \sin(\theta - x_1) \\ y = x_1 \end{cases}$$

For small errors, i.e.

$$\sin\left(\theta - \hat{\theta}\right) = \theta - \hat{\theta} \tag{5.12}$$

the following state space model is given

$$\begin{cases} \dot{x}_1 = K_1 \cdot K_2 \cdot (\theta - x_1) + x_2 \\ \dot{x}_2 = K_1 \cdot (\theta - x_1) \\ y = x_1 \end{cases} \Rightarrow \begin{cases} \dot{x}_1 = K_1 \cdot K_2 \cdot \theta - K_1 \cdot K_2 \cdot x_1 + x_2 \\ \dot{x}_2 = K_1 \cdot \theta - K_1 \cdot x_1 \\ y = x_1 \end{cases} \Rightarrow$$

$$\begin{cases} \dot{x} = \begin{bmatrix} -K_1 \cdot K_2 & 1 \\ -K_1 & 0 \end{bmatrix} \cdot x + \begin{bmatrix} K_1 \cdot K_2 \\ K_1 \end{bmatrix} \cdot u \\ y = \begin{bmatrix} 1 & 0 \end{bmatrix} \cdot x \end{cases} \tag{5.13}$$

and it will give the following linear transfer function

$$G_p(s) = \frac{\hat{\theta}(s)}{\theta(s)} = \frac{K_1(1 + K_2 s)}{s^2 + K_1 \cdot K_2 \cdot s + K_1} \tag{5.14}$$

which has the closed-loop system as seen in figure 5.7

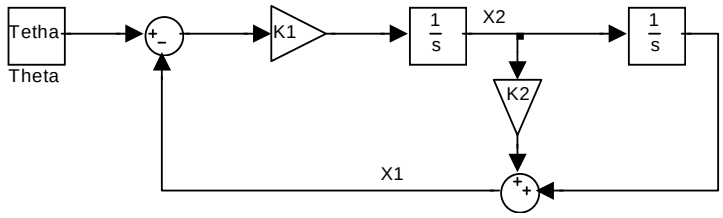

Figure 5.7. Linearized block model.

The denominator of $G_p(s)$ is the characteristic polynomial for the process, i.e.

$$s^2 + K_1 K_2 \cdot s + K_1 \tag{5.15}$$

By placing the roots of the polynomial in eq. (5.15), a convenient behaviour can be achieved. Comparing the polynomial to a general second order model is one way of determining K_1 and K_2. The general model has the form

$$G_m(s) = \frac{\omega_n^{\,2}}{s^2 + 2 \cdot \zeta \cdot \omega_n \cdot s + \omega_n^{\,2}} \tag{5.16}$$

where ω_n is the natural frequency of the closed-loop system and ζ is the damping factor. The coefficients of the polynomial in eq. (5.15) now becomes

$$K_1 = \omega_n^{\,2}$$
$$K_2 = \frac{2 \cdot \zeta}{\omega_n} \qquad (5.17)$$

To determine good values on K_1 and K_2, step responses from 80Hz to 40Hz are investigated with different values for ω_n and ζ, $\omega_n = [100\ 300\ 400]\,\text{rad/s}$ and $\zeta = [0.3\ 0.4\ 0.5]$. The step response behaviours are shown in figure 5.8a – 5.8c. During the simulation the input signals are noisy sinusoidal.

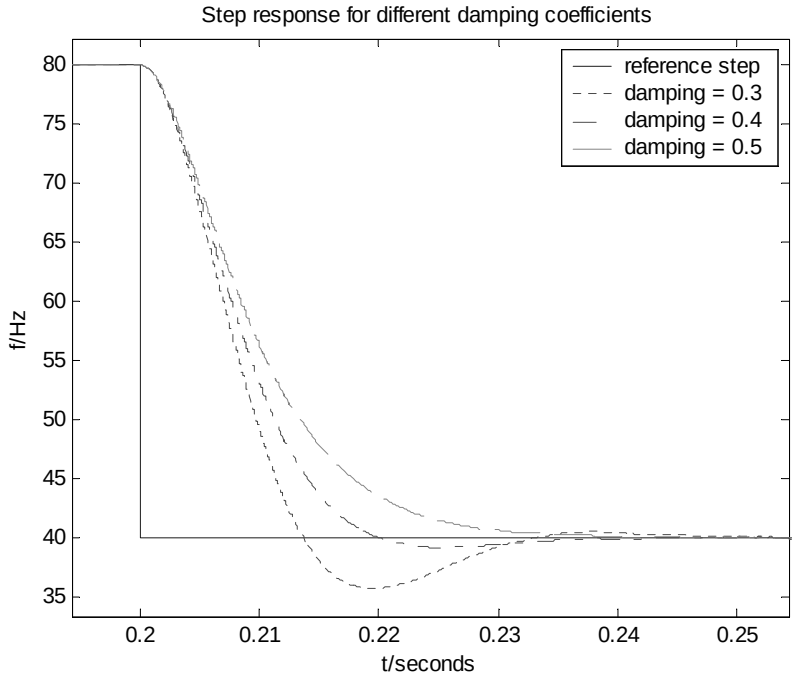

Figure 5.8a. Step response when $\omega_n = 100\text{rad/s}$ and $\zeta = [0.3\ 0.4\ 0.5]$.

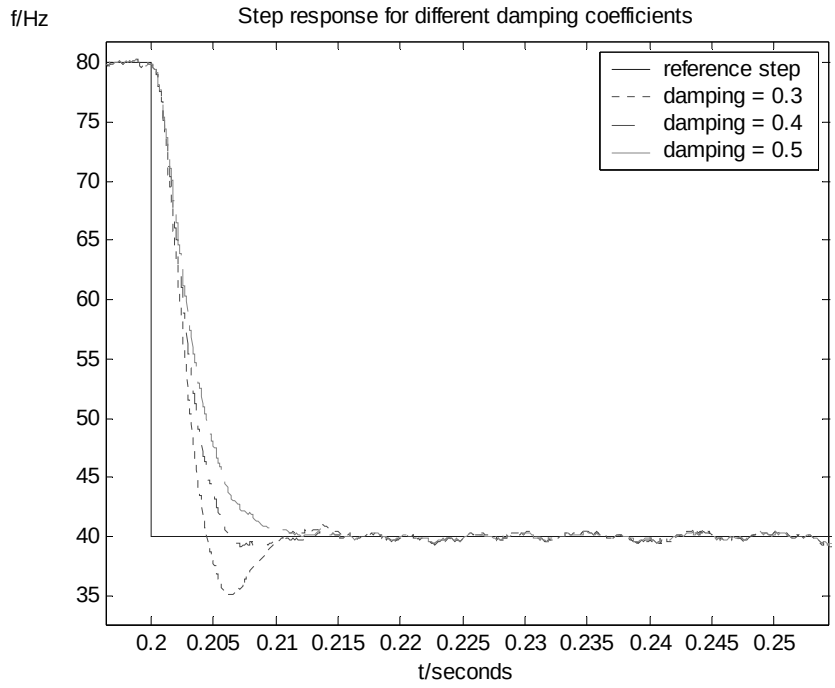

Figure 5.8b. Step response when $\omega_n = 300\text{rad/s}$ and $\zeta = [0.3\,0.4\,0.5]$.

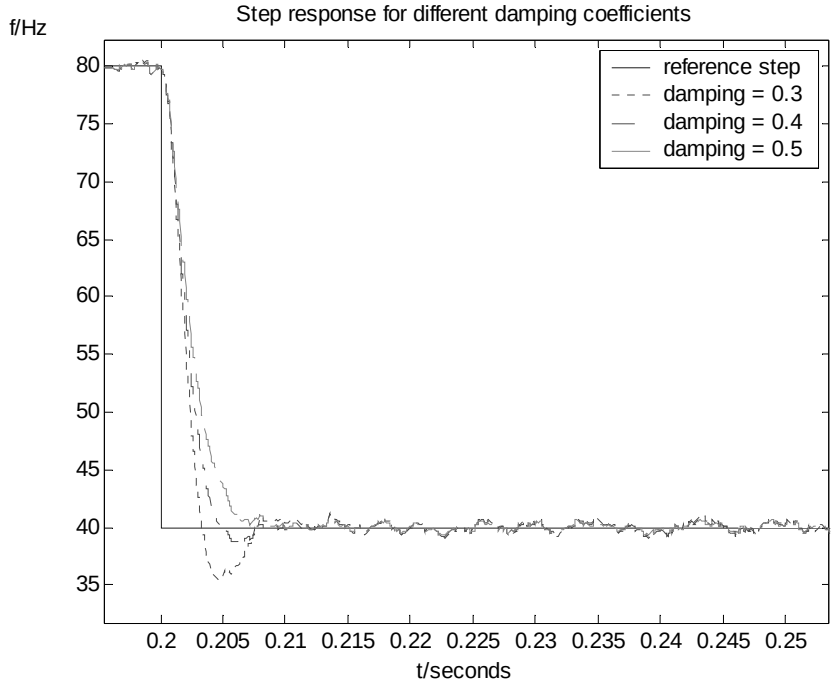

Figure 5.8c. Step response when $\omega_n = 400\text{rad/s}$ and $\zeta = [0.3\,0.4\,0.5]$.

As seen in figure 5.8a – 5.8c, different ζ and ω_n give different over-shoot and settling time. Some conclusions from these figures can be drawn:

- The damping factor ζ determines the over-shoot and therefore also affects the settling time of the step response, i.e. with small ζ more overshoot and oscillation is given.

- The natural frequency ω_n determines the settling-time of the step response, i.e. with large ω_n faster step response is given. A limitation of ω_n is, that if the signal is not clean (which of course it never is), with large ω_n more variation around the estimated mean value is given.

In figure 5.8a – 5.8c it is seen that suitable values are $\omega_n = 300\text{rad/s}$ and $\zeta = 0.4$, which mean fast settling time ($\approx 12\text{ms}$) and small oscillation ($\geq 5\%$) are given. It is also seen that if ω_n is large (i.e. in this example $\omega_n = 400\,\text{rad/s}$), the estimated speed fluctuates more around the correct value. This is because the noise influences the system more, i.e. the gain in the control loop becomes large ($K_1 \propto \omega_n^2$).

If $\omega_n = 300\,\text{rad/s}$, then an appropriate sampling time h has to be chosen. A rule of thumb[32] is $0.1 \leq \omega_n \cdot h \leq 0.6$. Also h has to be chosen to avoid aliasing. In figure 5.9 the step response with $h = 0.33\text{ms}$, $\zeta = 0.4$ and $\omega_n = 300\,\text{rad/s}$ is shown.

[32]Reference [15] p.130.

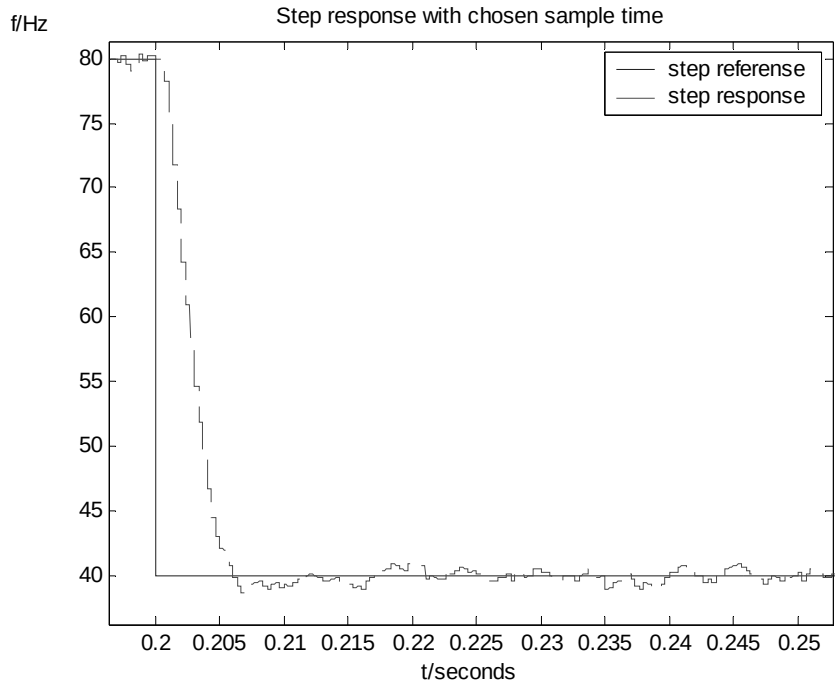

Figure 5.9 Step response with $\omega_n = 300\,\text{rad/s}$, $\zeta = 0.4$ and $h = 0.33\text{ms}$.

5.3. Tracking Demodulation- vs. Few Measurements methods

In figure 5.10 the step responses for Tracking Demodulation-, Few Measurement Variance- and Few Measurements method are shown. The Tracking Demodulation parameters are set to the most optimal, as in chapter 5.2.1. The sensor signals are noisy sinusoidal.

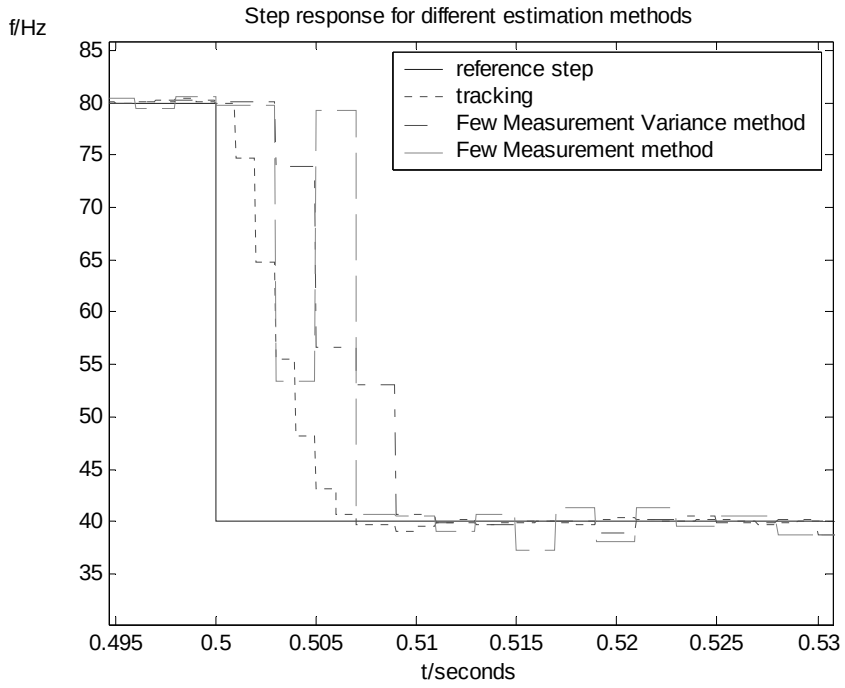

Figure 5.10. Step response for different estimation methods.

As seen in figure 5.10 the fastest and the most robust step response is achieved with the Tracking Demodulation method. One of the reasons why this method is faster is that it is independent of the estimated velocity. This because a sampling frequency not much faster than $\frac{1}{12}$ of the wheel speed frequency[33] is needed. Therefore the Few Measurements methods in the simulation in figure 5.10 are unable to perform a new estimate every millisecond, which is done by the Tracking Demodulation method.

Another advantage with the Tracking Demodulation method is that not so much pre-filtering is needed. The Few measurements methods are rather sensitive to noise compared to the Tracking Demodulation method. When implementing the different methods, the calculation time differs a lot from the different methods, especially the Few Measurements Variance method, which has a lot of time demanding calculations. This means that the method becomes slower.

[33] In figure 5.10 the sensor frequency is 40Hz, which results in an appropriate sampling frequency of 1/(12*40) s ≈ 2ms.

5.4 Summary

Zero detection is an easy and fast method for determine the wheel speed when driving at high velocities. As mentioned in chapter 4 this estimation is too slow at low speed, and therefore two other methods are investigated. These methods are Few Measurements- and Tracking Demodulation method. The Few Measurements method is a fast method, which uses three consecutive samples for determine the frequency of a single sinusoidal. This method needs rather clean signals, and therefore pre-filtering is needed. An improvement with this method is to make a fourth sample, and then compute two frequency estimates, which use the statistical dependency of these two estimates. Therefore more stable estimates are achieved.

The Tracking Demodulation method uses two sensors with a phase of 90 degrees between them. By making an estimation error between the correct- and estimated position, it is possible to estimate the wheel speed. Comparison of the Few Measurements- and Tracking Demodulation method shows that the Tracking Demodulation method is faster and more robust at low velocities, and is therefore suggested to be used. Another advantage is that Tracking Demodulation method actually ”tracks” the correct position, and could therefore be used to compensate for the wobble disturbance[34] and the fact that for different wheel speed, different amplitude in the sensor signal is obtained.

[34] See chapter 6.2.

6. Noise influence on- and filtering of the sensor signal and the frequency estimations

The output signal from the Solid-state sensors (which are used in the rapport) is a pulse-train[35]. Therefore that signal is less sensitive to noise. In this chapter, filtering of the Inductive Sensor signal from disturbances and the digital filters used in the simulations and implementations are discussed.

6.1. Filtering the analogue sensor signal

A big question that cannot be answered without real tests of the sensors is the level of noise in the output signal of the sensors. With the test rig described in chapter 7, test runs were made and test data from an Inductive sensor were logged into an oscilloscope. When the test rig was run with a frequency of 300 Hz[36], a raw sensor signal was attained. See figure 6.1.

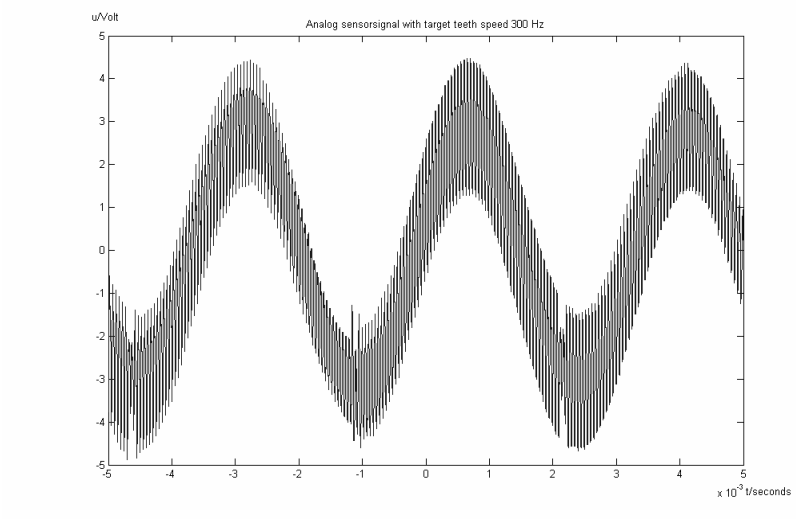

Figure 6.1. Unfiltered sensor signal.

In figure 6.1 it is shown that the senor signal has a very high-level frequency noise, which affects the “true” sensor signal. Because the noise is of high frequency compared to the frequencies that are to be detected, a simple

[35] See chapter 4.2.
[36] To transform the sensor frequency, see Appendix A.

analogue low pass filter is made. This filter may have a cut-off frequency at 10 kHz. It is shown that this is a safe cut off frequency[37] and that the real sensor signal never approaches this value. Using a filter with the transfer function

$$H(s) = \frac{1}{0.0001 \cdot s + 1} \tag{6.1}$$

the filtered signal in figure 6.2 is attained.

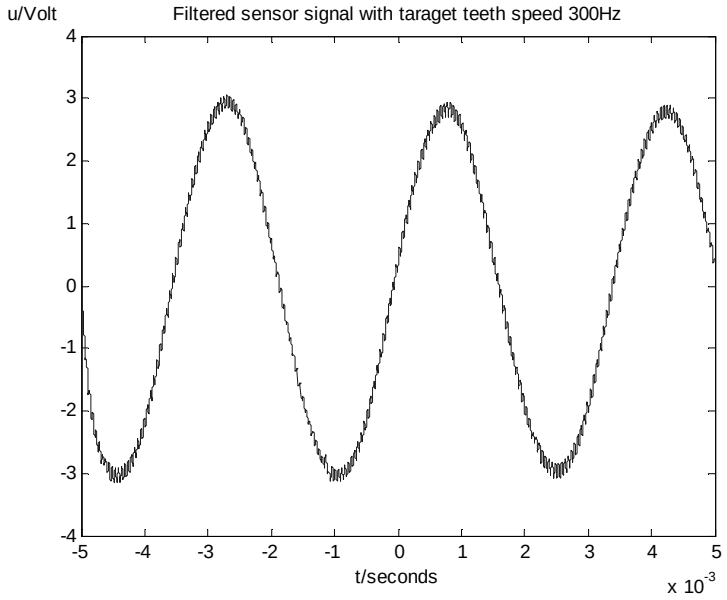

Figure 6.2. Filtered sensor signal.

This signal may be used to estimate the wheel speed[38].

[37] See chapter 5 and Appendix A. (A sensor frequency of 10 000 Hz means a vehicle speed of around 1200km/h, which will not be of any interest, when analysing ABS-brakes that are used in commercial vehicles.)
[38] To improve the signal even more an MA-filter can be added.

6.2. The Wobble disturbance

When a real target wheel in a test rig[39] or in a vehicle is used, a disturbance is received that varies due to the distance (air gap) between the sensor and the target wheel. This is shown in the measured signal as changing amplitude maximum and minimum, although travelling at the same velocity. See figure 6.3. The disturbance (called a wobble disturbance) has come up because of uneven distance between sensor and target wheel, which varies periodically.

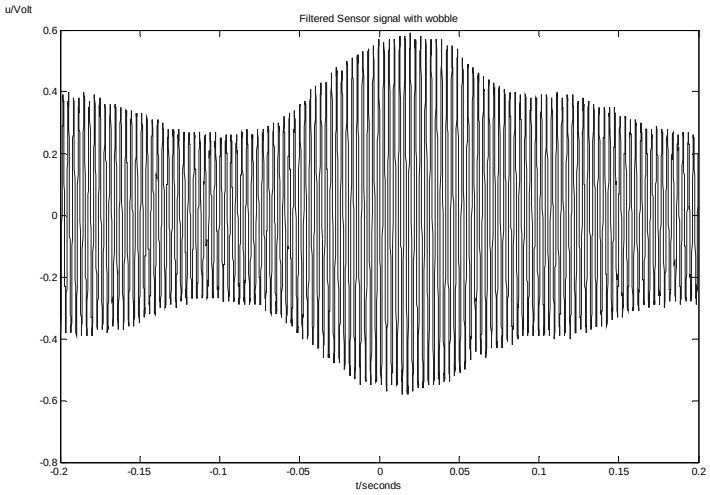

Figure 6.3. Sensor signal with wobble.

Problems in the A/D-converter[40] are due to this disturbance, i.e. maximum resolution cannot always be obtained. Also when using the Tracking Demodulation method (i.e. two sensors) on the test rig, i.e. different spacing between the two sensors and the target wheel, which results in large differences in the amplitude of the sensor signals are attained, due to the distance between the sensors[41]. This results in violating the linearization in eq. (5.12) of the closed loop system in eq. (5.13). To avoid the wobble disturbance in the estimations, a peak-detection has to be made, i.e. how the maximum/minimum values change over one turn of the wheel. Then a compensation of the signal can be made through amplification.

[39] See chapter 7.
[40] See chapter 8.
[41] See figure 7.2 in chapter 7.

6.3. ARMA-filters

When a momentary value is received, some sort of filtering is needed when running on a real process. Appropriate filters are the ARMA-filters, because they are easy to implement. The structure of an ARMA-filter[42] is

$$H(z) = \frac{B_q(z)}{A_q(z)} = \frac{\sum_{k=0}^{q} b_q(k) \cdot z^{-k}}{1 + \sum_{k=0}^{q} a_q(k) \cdot z^{-k}} \qquad (6.2)$$

6.3.1. AR-filter

To avoid unrealistic changes in the velocity estimations, a digital low-pass filter of an AR-structure is used. This is an ARMA-filter with $B_q = b(0)$, i.e.

$$H(z) = \frac{b(0)}{1 + \sum_{k=0}^{q} a_q(k) \cdot z^{-k}} \qquad (6.3)$$

By choosing an appropriate cut-off frequency the AR-filter improves the estimations.

6.3.2. MA-filter

Whenever there is time on the real process a convenient way to improve the estimations is to use some sort of averaging filter, e.g. a MA-filter. This is an ARMA-filter with $A_q = 1$, i.e.

$$H(z) = \sum_{k=0}^{q} b_q(k) \cdot z^{-k} \qquad (6.4)$$

Combining this filter with an AR-filter the estimated value can be improved a

[42] See reference [9].

lot. The MA-filter can be used when reducing the noise from the sensor signal, but also to achieve better speed estimation.

6.4 Summary

When real tests and implementations of the different wheel speed estimations have been performed on the real test rig, filtering is needed. The inductive sensor signal has a high frequency component added to the ”true” frequency, and therefore an analogue low pass filter is added as a pre-filtering. The wobble disturbance could give problems, and has to be taken under consideration. When ether there is time in an implementational aspect, the ARMA-filters are one way to stabilize, both in the A/D-conversion, and when an estimated velocity is obtained.

7. Real sensor testing

In this chapter the test rig, which was used in the project, is described. Haldex Brake Products AB has supplied the master theses project with this test rig, see figure 7.1. On the test rig, real tests of different type of sensors are carried out.

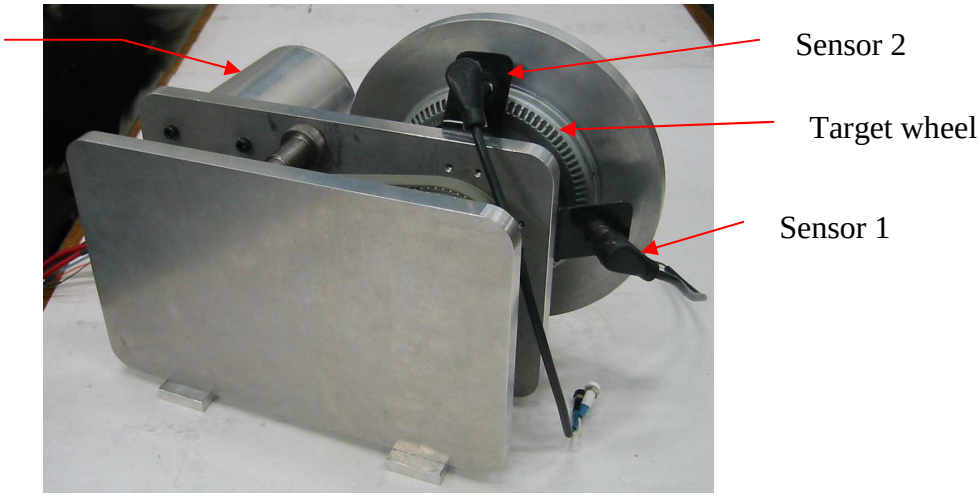

Figure 7.1. Picture of the test rig.

On this rig, sensor 1 has been set to 0 degree reference angle. This means that sensor 2 has been placed with an approximate angel of 90-degree angle compared with sensor 1.

An electrical motor is used to drive the “wheel”. The revolutions of the electrical motor are then used to drive the “wheel” via a coupling. The coupling has a gear ratio of approximately 20:1. This gives a target wheel pulse range between approximately 15 Hz to 500 Hz, which could be translated into 1.8 km/h to 60 km/h, if the wheel has a radius of 0.5 meter. When the lower limit is reached, the motor cannot turn the wheel anymore due to friction that serves as a resistance. When reaching the upper limit the supply circuits to the motor cannot deliver any more power.

The electrical motor also has an optical sensor that measures the speed of the motor. With knowledge of the gear ratio this sensor could be used as a reference speed signal.

As seen in figure 7.2 the sensors could be placed with different lengths from the target wheel.

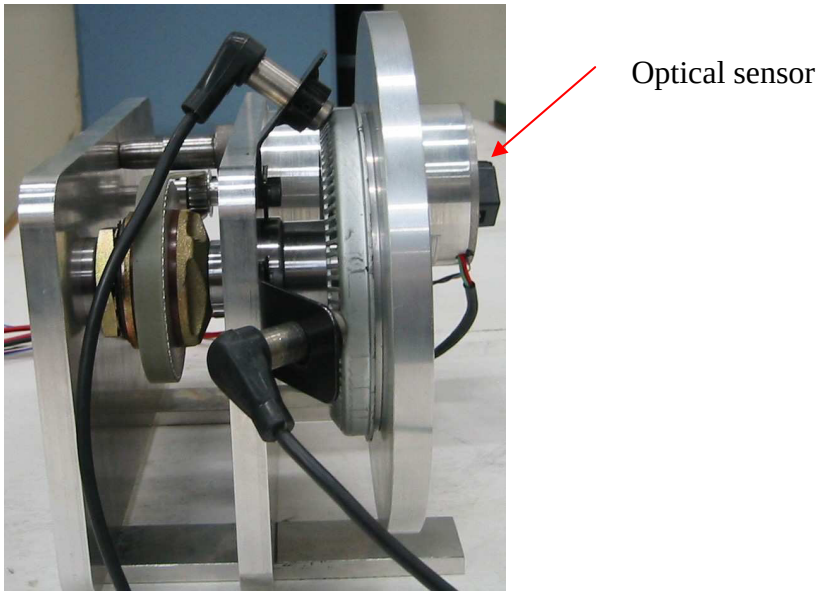

Figure 7.2. Picture of the sensor position towards the target wheel.

In all the tests carried out, the sensors have been placed as close as possible, i.e. the sensors should not touch the target wheel.

8. Implementation methods into a microcontroller

In this chapter the implementation of zero detection and few measurements method into a microcontroller are discussed. General description of the microcontroller, and different aspects of what is needed to be considered when the methods are implemented, is brought up.

8.1. The microcontroller

A motor control development card has been put to our disposal. This card is equipped with a microcontroller. This processor can be run at clock frequencies up to 40 MHz. It contains several useful things that can be used in an application like this, e.g. digital signal processor, 10 and 12-bit A/D-converter. It also contains CAN (Controller Area Network), SPI (Serial Peripheral Interface), UART (Universal Asynchronous Receiver-Transmitter) and I2C (Integrated Circuit) interface. These interfaces can be used to communicate with other processors or devices that need information about the result of the velocity calculation. The circuit also has five timers and several ports that can be used as interrupts. After each interrupt a certain code can be executed.

The processor is easily programmed with the aid of MPLAB (Microchips programming interface), which also contains software simulator. This software simulator can be used to verify the functionality of the project before downloading it into the circuit.

8.2. Pre-signal processing for Inductive sensors

A restriction that can arise when using the A/D-converter in the micro controller is that it is only possible to A/D-convert voltage levels between Vdd and Vcc supplied to the circuit, in this case 0 and 5V. This means that with an inductive sensor, only half of the period would be A/D-converted correctly. The negative part would be A/D-converted to zero. A

transformation of the sensor signal is made to solve this problem. In figure 8.1 a block diagram of the transformations steps, used to get a correct sensor signal into the circuit, is shown.

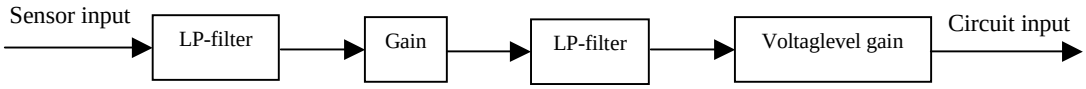

Figure 8.1. Signal processing block diagram.

As pointed out in chapter 6 the raw sensor signal has a high-level signal noise, which has to be filtered before any other activity takes place, therefore a low pass filter with a cut-off frequency at 10 kHz alters the signal first. The low pass filter is (as mentioned before) safe to use, without risking to block the useful information of the sensor signal.

After this a gain (amplifier) of the signal is made[43]. This is done so that even a small amplitude signal at low speeds will use as much of the A/D-converter resolution as possible. Otherwise, at low speed measurement, the signal would be of such low amplitude that changes in amplitude might not be detected. This gain step has to be an active gain. This means that it has to change its gain for different velocities (i.e. frequencies). After this step a new low pass filtering with the same cut-off frequency as before is used, this due to the amplifier also gains the remaining noise components from the first low-pass filter.

The last step is to add a DC voltage to the sinusoidal AC voltage[44]. This DC voltage has to be large enough to raise the zero level from zero voltage to (Vcc-Vdd)/2. This level will act as a virtual zero voltage level in the circuit. This means that if the result from the A/D-converter is set to be a signed number, 0 volt will be returned when the input reaches (Vcc-Vdd)/2.

[43] The amplifier is an inverted operational amplifier, designed as in reference [8].
[44] This applied DC-voltage is could be obtained with a so called ”lock circuit”. See reference [8].

During implementation test using the test rig[45] and the microcontroller, the following circuit solution in figure 8.2 was used to alter the inductive sensor signal, so it could be used by the microcontroller.

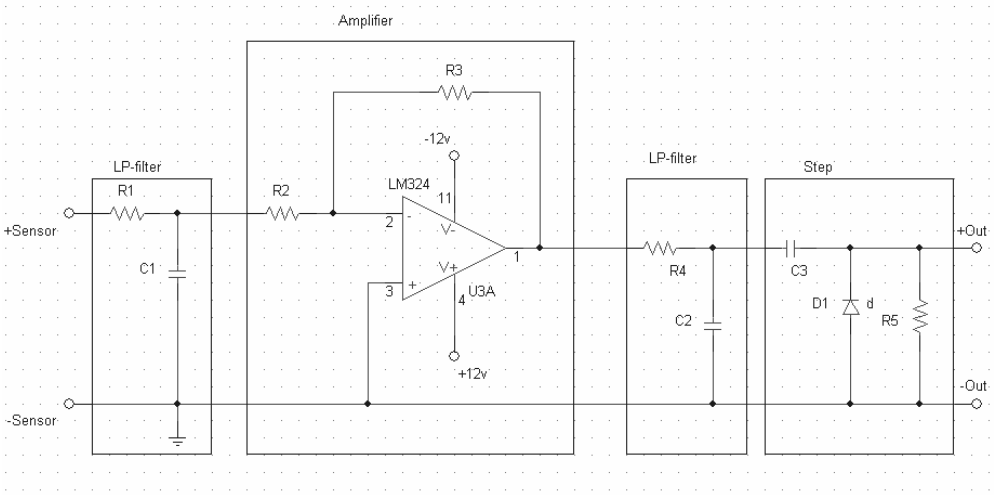

Figure 8.2. Circuit solution.

8.3. General implementation ideas

When implementing any of the methods into the circuit, there are certain things that have to be thought of to get as good result as possible:

- *Periodic sampling with the use of timers or interrupts.* Each estimation method has different algorithms and constraints when an A/D-sample has to be made. The common denominator is that all samples has to be made as close as possible to the required sample time of the method.

- *Priority level of the different interrupts.* If there are at least two interrupts of any sort, e.g. if one timer interrupt calculates an average of a few older velocity calculations, and the other which makes an A/D-sample of a sensor. Then a good way would be to have a higher priority on the second interrupt. This because of time readings in the

[45] Described in chapter 7

A/D-conversion interrupt, which would be affected by interrupts, resulting in a greater time value than it should have.

- *Calculation optimisation.* Depending on the circuit used, and programming language used, a calculation can take different amount of time. E.g. in the math library that is used in C, a multiplication or a division could take quite a long time. This is because methods are implemented with the use of recursive or iterative numerical functions. In this circuit using the DSP-functions could solve this problem, and make the calculations somewhat less time-consuming.

In the following pages, the structures, which were used to implement velocity measurement using Hall-Effect sensor, and also analogue inductive sensor with the method of Few Measurements methods, are shown.

8.4. Implementation of Few Measurements method

In figure 8.3 – 8.4, the charts of how Few Measurements method was implemented into the microcontroller to measure velocity with an inductive sensor, is shown. This implementation contains two tasks; a main task that executes all the time, and one periodic task, which executes so often that 12 samples per sinusoidal period is achieved. Each sample is an average of 6 samples, which means that a sample period of 72 times the sinusoidal frequency should be used to achieve the best result.

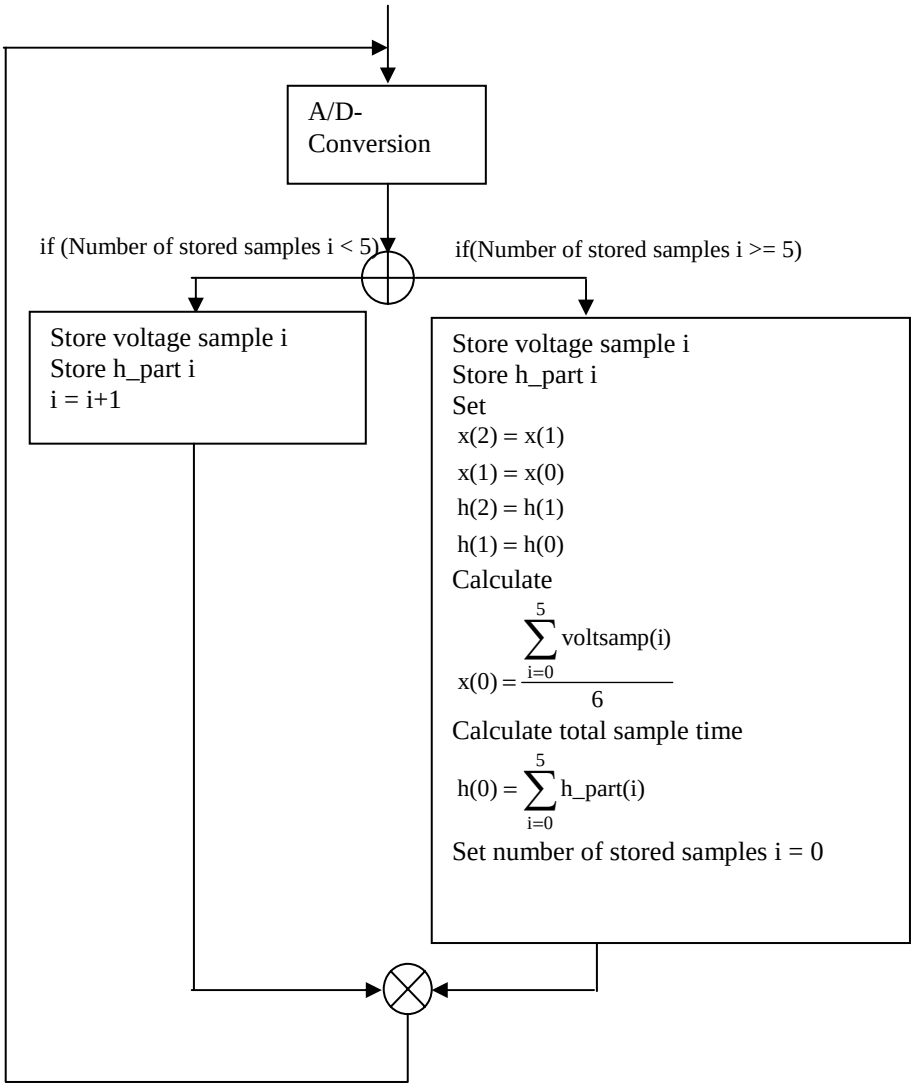

Figure 8.3. Implementation chart for the A/D-conversion procedure.

The A/D-conversion task is, as mentioned, a periodic task that samples the sensor signal 72 times during one period, when it is used optimally. The task has been implemented with a timer that counts the correct number of clock ticks before making an interrupt. When an interrupt is made, the chart in figure 8.3 is executed. This task has been set to have the highest priority. This is to hinder other tasks from interrupting this task, thus making the readings as correct as possible.

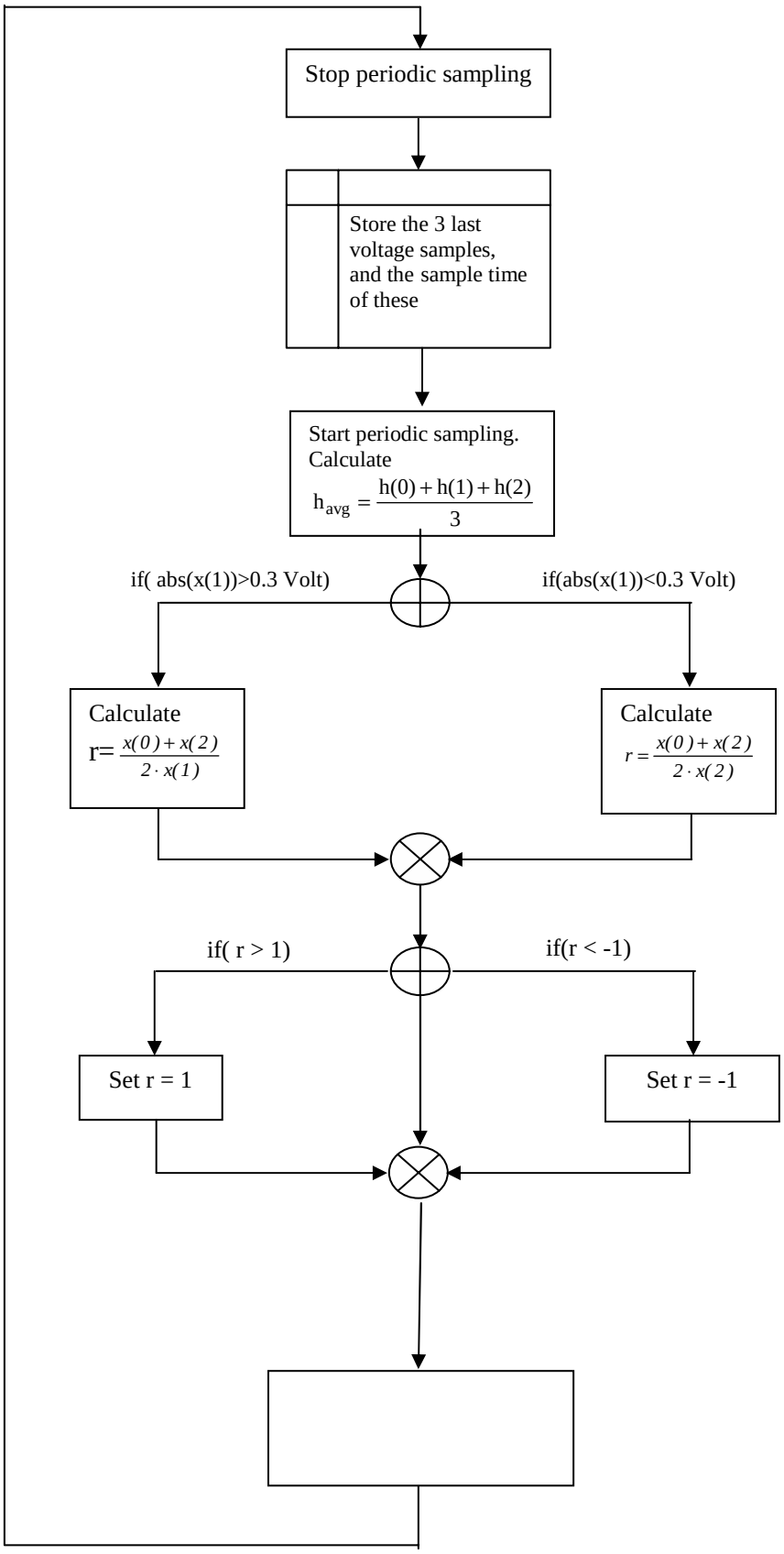

Figure 8.4. Implementation chart for the main calculation procedure.

The task in figure 8.4 is placed in main, which means that it is executing whenever the sampling task is not. One stoppage is made on the A/D-conversion task. This is done when the calculation loop reads new values to base its calculations on. If a stoppage is not made, this could mean that the A/D-conversion loop could break, and modify the variables that the main task is about to read, resulting in a calculation result that might be wrong.

8.5. Implementation of Hall-Effect sensor measurement

In figure 8.5 the chart of how Hall-Effect sensor signals can be measured by the microcontroller is shown. The loop in this figure is the main task and will execute all the time. Of course this does not take any of the above-mentioned points about sample time and priority under consideration. The choice of allowing this task to execute all the time is, because of the nature of the digitised signal that a Hall-Effect sensor delivers. It changes (as mentioned) from 0 volt to e.g. 5 volt, at the point when a sinusoidal period changes from negative to positive value (zero crossing). The opposite happens at a positive to negative value change. This loop then allows the processor to catch a change as close as possible.

If the sampling would instead have been put into a periodic sampling, then there could be a jitter in the time measurement, which would then turn up in the calculated velocity calculation as a variation in velocity that would be larger than it should be.

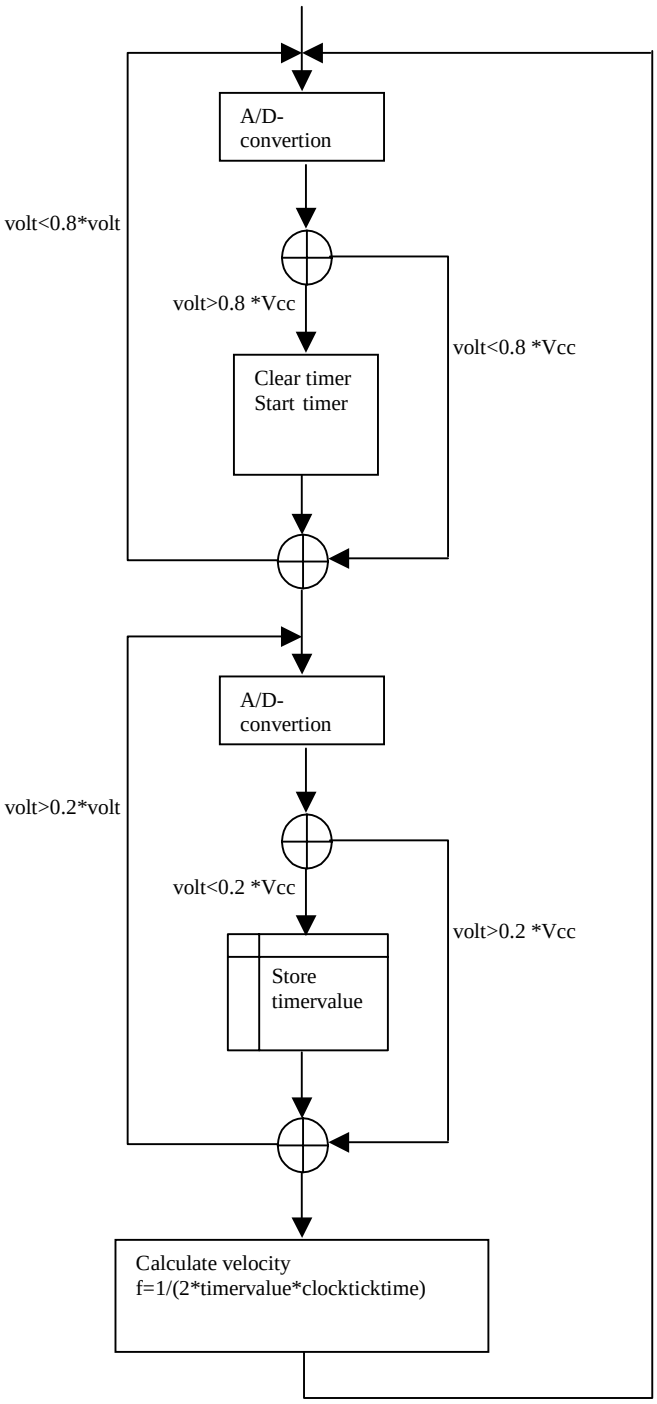

Figure 8.5. Implementation chart for Hall-Effect sensor estimation procedure.

8.6 Summary

When the estimation methods are implemented there are some common factors that have to be considered. First, it is necessary to use periodic sampling, which is carried out with the help of timers or interrupts[46] in a microcontroller, because of the importance to obtain samples as often as the required sample time. Second, the time demanding calculations in the estimation methods, e.g. multiplications and divisions, have to be optimized to minimize the calculation time.

[46] If there are more than one interrupt, it is suggested to have different priority of these interrupts.

9. Conclusions

As discussed in the rapport, problems arise when trying to achieve correct velocity estimation below 20 km/h. When using an inductive sensor, the first problem that occurs is that the amplitude level of the signal is too low. This means that the signal is very sensitive to noise and may give faulty velocity estimations when zero detection algorithms are used. A faulty zero might be detected.

It is proposed to use a first order filter to get rid of the noise, and an active amplifier will amplify the signal with different gain, determined by the current frequency of the target wheel, and current distance between sensor and target wheel. A Hall Effect sensor can be used to get around this problem. This sensor gives a good, stable signal that changes between low and high state, as the teeth of the target wheel pass by. But also, this sensor has problems below 20 km/h. In this case, the problem is that the time between states changes at these speeds start to rise to such values that it will be impossible to calculate velocity estimation within demanded deadlines.

By using either Few Measurement Estimation with or without variance compensation or Tracking Demodulation, which both have been presented in the rapport, faster wheel speed estimations are achieved. These methods use the inductive sensor. It will be possible to calculate new frequency estimations at least every $\frac{1}{12}$ of a period. This will then give possibilities to achieve valid frequency estimations below 20 km/h. These methods will also give a better estimate, because several estimations can be made within deadline and an average of these estimations can be calculated.

Comparisons between these two methods have been made. These show that better estimations are achieved with the Tracking Demodulation than the Few Measurements methods. Another advantage of Tracking Demodulation is that it has less time consuming calculations than the Few Measurements.

A disadvantage of the Tracking Demodulation method is that two inductive sensors have to be used, and these two have to be placed in a 90 degree angle.

As a conclusion from these comparisons, a suggestion is that velocity measurement shall be made by scheduling the use of the methods. At velocities above 20 km/h, zero detection could be used. Then, if two inductive sensors are used, these can be used to achieve an average value between these two sensors. Below 20 km/h it is suggested that Tracking Demodulation shall be used, instead of Few Measurement. Mainly because it is less time consuming when calculations are made, and it is independent of the wheel speed which the other methods are not.

Finally we would like to thank Haldex Brake Products which gave us the opportunity to do this master thesis project. We would especially like to thank Ola Nockhammar, the supervisor of this project, for his insightful thoughts and ideas which encouraged and inspired us. Thanks also to Anders Rantzer, our supervisor at the Department of Automatic Control, Lund Institute of Technology.

Appendix A

A.1. Wheel velocity

Vv=(Ov/(2*pi*N))*fs=((2*pi*rv)/(2*pi*N))*fs=(rv/N)*fs						
fs	Vv (m/s)	Vv (km/h)	rv = 0,5 meter	fs	Vv (m/s)	Vv (km/h)
30	0,98	3,54	N = 96	330	10,81	38,92
40	1,31	4,72		340	11,14	40,10
50	1,64	5,90		350	11,47	41,28
60	1,97	7,08		360	11,79	42,46
70	2,29	8,26		370	12,12	43,64
80	2,62	9,44		380	12,45	44,82
90	2,95	10,61		390	12,78	46,00
100	3,28	11,79		400	13,10	47,18
110	3,60	12,97		410	13,43	48,35
120	3,93	14,15		420	13,76	49,53
130	4,26	15,33		430	14,09	50,71
140	4,59	16,51		440	14,41	51,89
150	4,91	17,69		450	14,74	53,07
160	5,24	18,87		460	15,07	54,25
170	5,57	20,05		470	15,40	55,43
180	5,90	21,23		480	15,73	56,61
190	6,22	22,41		490	16,05	57,79
200	6,55	23,59		500	16,38	58,97
210	6,88	24,77		510	16,71	60,15
220	7,21	25,95		520	17,04	61,33
230	7,53	27,13		530	17,36	62,51
240	7,86	28,31		540	17,69	63,69
250	8,19	29,48		550	18,02	64,87
260	8,52	30,66		560	18,35	66,05
270	8,85	31,84		570	18,67	67,22
280	9,17	33,02		580	19,00	68,40
290	9,50	34,20		590	19,33	69,58
300	9,83	35,38		600	19,66	70,76
310	10,16	36,56		610	19,98	71,94
320	10,48	37,74		620	20,31	73,12

Table A.I. Transformation table from sensor frequency to vehicle speed.

Appendix B

B.1. Proof of Few Measurement method

With a signal as $x(t) = A \cdot \cos(\omega \cdot t + \theta)$ it is possible to derive an estimate as

$$r = \cos(\omega \cdot T) \Rightarrow \omega = \frac{\arccos(r)}{T}.$$

This can be done if the three consecutive samples are

$$x[0] = A \cdot \cos(\theta)$$
$$x[1] = A \cdot \cos(\omega \cdot T + \theta)$$
$$x[2] = A \cdot \cos(\omega \cdot 2 \cdot T + \theta)$$

which results in

$$r = \frac{x[0] + x[2]}{2 \cdot x[1]} = \frac{A \cdot \cos(\theta) + A \cdot \cos(\omega \cdot 2 \cdot T + \theta)}{2 \cdot A \cdot \cos(\omega \cdot T + \theta)} = \frac{A \cdot (\cos(\theta) + \cos(\omega \cdot 2 \cdot T + \theta))}{A \cdot (2 \cdot \cos(\omega \cdot T + \theta))} \Rightarrow$$

$$= \frac{\cos(\theta) + \cos(2 \cdot T\omega) \cdot \cos(\theta) - \sin(2 \cdot T \cdot \omega) \cdot \sin(\theta)}{2 \cdot \cos(\omega \cdot T) \cdot \cos(\theta) - 2 \cdot \sin(\omega \cdot T) \cdot \sin(\theta)} = \begin{bmatrix} \sin(2 \cdot T \cdot \omega) = 2 \cdot \sin(T \cdot \omega) \cdot \cos(T \cdot \omega) \\ \cos(2 \cdot T \cdot \omega) = 2 \cdot \cos^2(T \cdot \omega) - 1 \end{bmatrix} =$$

$$= \frac{\cos(\theta) + 2 \cdot \cos^2(T \cdot \omega) \cdot \cos(\theta) - \cos(\theta) - 2 \cdot \sin(T \cdot \omega) \cdot \cos(T \cdot \omega) \cdot \sin(\theta)}{2 \cdot \cos(T \cdot \omega) \cdot \cos(\theta) - 2 \cdot \sin(T \cdot \omega) \cdot \sin(\theta)} =$$

$$= \frac{2 \cdot \cos(T \cdot \omega) \cdot (\cos(T \cdot \omega) \cdot \cos(\theta) - \sin(T \cdot \omega) \cdot \sin(\theta))}{2 \cdot (\cos(T \cdot \omega) \cdot \cos(\theta) - \sin(T \cdot \omega) \cdot \sin(\theta))} = \cos(T \cdot \omega) \quad \underline{\text{FINISHED}}$$

References

[1]. Adelson Ronald M., *Frequency Estimation from Few Measurements*, 1997, Academic Press, Journal: Digital Signal Processing

[2]. AI-Tek Instruments Inc., *Sensors*, http://www.aitekinstruments.com/pdf/sensors.pdf , 2003-07-07

[3]. Cheng David K., *Field and Wave Electromagnetics, Second Edition*, 1992, Addison Wesley Publishing Company Inc, ISBN 0-201-12819-5

[4]. Dietmayer Klaus ,Schmeiβer Fritz, *Rotational Speed Sensors KMI15/16*, 1999, Philips Electronics N.V., http://www.semiconductors.philips.com/acrobat/applicationnotes/KMI16-15.pdf , 2003-10-28

[5]. Honeywell, *Hall Effect Sensing and Application*, MICRO SWITCH Sensing and Control, http://content.honeywell.com/sensing/prodinfo/solidstate/technical/hallbook.pdf , 2003-10-28

[6]. Lequesne B. , Pawlak A. , Schroeder T., *Magnetic velocity sensors*, 1991, IEEE, Journal: Industry Applications Society Annual Meeting, 1991., Conference Record of the 1991 IEEE

[7]. Limpert Rudolf, *Brake Design and Safety, Second Edition*, 1999, Society of Automotive Engineers, Inc., ISBN 1-56091-915-9

[8]. Lundqvist Hans, *Analog kretselektronik*, 1992, Liber Utbildning, ISBN 91-634-1551-8

[9]. Monson Hayes, *Statistical digital signal processing and modeling*, 1996, John Wiley, ISBN 0-47-159431-8

[10]. Morgan Don, *Tracking Demodulation*, 2001-02-26, www.embedded.com, http://www.embedded.com/story/OEG20010221S0089 , 2003-10-28

[11]. Proakis John G., Manolakis Dimitris G., *Digital Signal Processing, Principles, Algorithms, and applications Third edition*, 1996, Prentice-Hall Inc., ISBN 0-13-394289-9

[12]. Robert Bosch GmbH, *Brake Systems for passenger cars, second edition*, 1995, Robert Bosch GmbH

[13]. Slotine E. Jean-Jacques,Weiping Li, *Applied Nonlinear Control*, 1991, Prentice-Hall Inc., ISBN 0-13-040890-5

[14]. Wong J.Y. , *Theory of ground vehicles*, 2001, John Wiley & Sons Inc. , ISBN 0-471-35461-9

[15]. Åström Karl J. Björn Wittenmark, *Computer-Controlled Systems Theory and Design, Third Edition*, 1997, Prentice-Hall Inc., ISBN 0-13-314899-8